Sulfur-Doped Graphene *via* Thermal Exfoliation of Graphite Oxide in H_2S, SO_2, or CS_2 Gas

Hwee Ling Poh,[†] Petr Šimek,[‡] Zdeněk Sofer,[‡] and Martin Pumera[†,*]

[†]Division of Chemistry & Biological Chemistry, School of Physical and Mathematical Sciences, Nanyang Technological University, Singapore 637371, Singapore, and
[‡]Department of Inorganic Chemistry, Institute of Chemical Technology, 166 28 Prague 6, Czech Republic

ABSTRACT Doping of graphene with heteroatoms is an effective way to tailor its properties. Here we describe a simple and scalable method of doping graphene lattice with sulfur atoms during the thermal exfoliation process of graphite oxides. The graphite oxides were first prepared by Staudenmaier, Hofmann, and Hummers methods followed by treatments in hydrogen sulfide, sulfur dioxide, or carbon disulfide. The doped materials were characterized by scanning electron microscopy, high-resolution X-ray photoelectron spectroscopy, combustible elemental analysis, and Raman spectroscopy. The ζ-potential and conductivity of sulfur-doped graphenes were also investigated in this paper. It was found that the level of doping is more dramatically influenced by the type of graphite oxide used rather than the type of sulfur-containing gas used during exfoliation. Resulting sulfur-doped graphenes act as metal-free electrocatalysts for an oxygen reduction reaction.

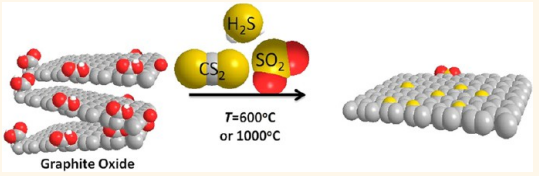

KEYWORDS: graphene · doping · sulfur · gas phase · electrochemistry

Graphene in its pure state has been shown to exhibit many interesting materials properties that are useful for electronic and electrochemical application, such as nanoelectronics and electrode surfaces (*i.e.*, oxygen reduction reaction or electrocatalysis).[1−7] However, the suitability of the material for these applications is limited by the fact that pristine graphene exhibits zero band gap[8] and that its electrochemical behavior resembles that of graphite.[9] Doping of graphene with various atoms, such as transitions metals,[10,11] halogens,[12−14] hydrogen,[15] nitrogen,[16−20] or sulfur[21] can change the electron density[22] in the graphene sheet and provide an electrocatalytic surface in the material at the same time.

Sulfur doping of graphene is of particular interest as the resulting materials are expected to have a wider band gap due to the electron-withdrawing character of sulfur. Previous studies have successfully produced elemental sulfur/graphene composites by mechanically mixing the individual components[23,24] or heating graphene with benzyl disulfide where the creation of sulfur-epoxy bonds in graphene was proposed to exist.[21] Here we have employed different sulfur doping strategies and we investigated to what extent they influence the composition of the final product. We used graphite oxide as a starting material, which was then thermally exfoliated in a sulfur-containing gaseous environment (Scheme 1). Graphite oxide was prepared using three different classical methods, such as Staudenmaier,[25] Hofmann,[26] and Hummers[27] and further exfoliated at high temperature in SO_2, H_2S, and CS_2 gas atmosphere. Interestingly, we observed that the type of graphene oxide used for sulfur doping brought about a greater effect on the properties of the final product as compared to the type of the sulfur-containing gas used for exfoliation. We show that sulfur-doped graphenes show electrocatalysis for the oxygen reduction reaction, which is of high industrial importance, and make them ideal candidates for metal-free oxygen reduction electrocatalysts.

RESULTS AND DISCUSSION

To prepare sulfur-doped graphenes, graphite was first oxidized to graphite oxide with (a) fumic nitric acid, H_2SO_4, and $KClO_3$

* Address correspondence to pumera@ntu.edu.sg.

Received for review February 28, 2013 and accepted May 6, 2013.

Published online May 08, 2013
10.1021/nn401296b

© 2013 American Chemical Society

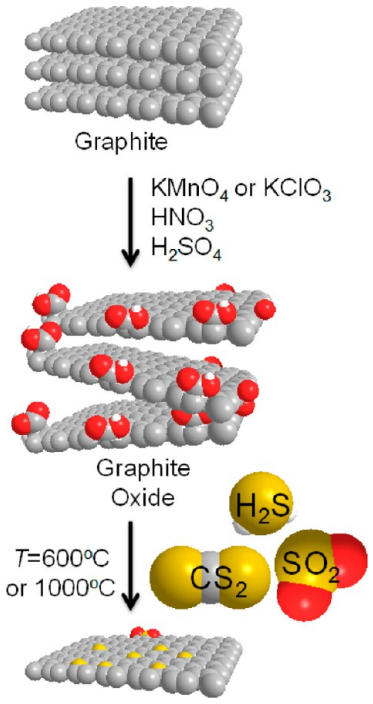

Scheme 1. Fabrication of sulfur-doped graphene by thermal exfoliation of graphite oxide prepared by Staudenmaier, Hofmann, and Hummers method in CS_2, H_2S, or SO_2 atmospheres.

(Staudenmaier method (ST)), (b) 68% HNO_3, H_2SO_4, and $KClO_3$ (Hofmann method (HO)), or (c) H_2SO_4, $KMnO_4$, and $NaNO_3$ mixture (Hummers method (HU)). Consequently, the material was placed in a quartz tube and exfoliated in SO_2, H_2S, or CS_2 atmospheres (1000 mbar) at 600 or 1000 °C. The resulting materials were then extensively characterized using scanning electron microscopy (SEM), high-resolution X-ray photoelectron spectroscopy (HR-XPS), Raman spectroscopy, and combustible elemental analysis. Its other properties such as ζ-potential and conductivity were also investigated. The materials discussed in this paper are labeled in accordance with the reaction conditions and types of materials used; that is, HO-S: [CS_2/1000 °C] signifies sulfur-doped graphene prepared from Hofmann graphite oxide exfoliated in CS_2 atmosphere at 1000 °C. The thermally reduced graphene oxide (TRGO) starting materials that are not doped with sulfur will be indicated as ST, HO, and HU which represents Staudenmaier TRGO, Hofmann TRGO, and Hummers TRGO, respectively.

Materials Characterization. The following sections will further elaborate in detail the findings obtained for these materials using various characterization techniques such as scanning electron microscopy, Raman spectroscopy, and X-ray photoelectron spectroscopy (XPS). Comparison will also be made with non-sulfur-doped graphene oxides (ST, HU, and HO) which act as the control materials in this paper.

Characterization of the materials was first carried out using SEM to observe the morphology and topographical details. Imaging of the materials was carried out at various magnifications of 370×, 6000×, 10 000×, and 50 000×, as shown in Figure 1. It was observed from the obtained images that all of the materials have been successfully exfoliated as the images presented structures that are similar to exfoliated graphene oxides where separated sheets of sulfur-doped graphene oxides could be clearly observed. Comparison between different starting materials, sulfur sources, or reaction conditions showed that no major structural differences could be visually observed from the different conditions that were executed to generate the materials.

Further structural information such as the density of defects in the materials can be accomplished using Raman spectroscopy technique through the determination of the G (related to pristine sp^2 graphitic layer) bands at ~1560 cm^{-1} and D (related to defect in sp^2 lattice) bands at ~1350 cm^{-1} in the spectrum. The presence of defects in the pristine graphene structure is crucial in affecting the electrochemical behavior of the materials as earlier studies have shown that such reactions are most likely to occur at these sites of defects which are characterized to be of a sp^3 nature. Using the green Ar laser source at 514 nm, a Raman spectrum which shows the presence of a D and G band is recorded. The density of defects can be represented by a calculated D/G ratio of the intensity of the D band to the intensity of the G band where this ratio is an indication of the degree of disorder in the structure. Figure 2 shows the Raman spectra for corresponding sulfur-doped as well as for undoped (graphite oxide exfoliated in argon atmosphere) graphenes. The calculated D/G ratios for the Staudenmaier materials are 0.77 for the undoped ST thermally reduced graphene oxide, 0.62 for sulfur-doped Staudenmaier graphene oxide using the H_2S source at 600 °C (labeled as ST-S: [H_2S/600 °C]), and 0.69 for ST-S: [SO_2/600 °C] (refer to Figure 2A,D). The formation of defects in these ST graphene oxides may be partially attributed to the sulfur that is being doped onto the graphene oxide surfaces. Derivation of the average crystalline size (L_a) of the materials can also be possible through the use of the D/G ratios in the equation as follows:[28]

$$L_a = 2.4 \times 10^{-10} \times \lambda_{laser}{}^4 \times I_G/I_D$$

The I_G/I_D is the ratio of the intensities of the G and D bands, respectively, and λ_{laser} refers to the laser wavelength (nm) used in the measurement of the Raman spectrum (*i.e.*, 514 nm). The calculated L_a values are 21.7 nm for ST, 27.1 nm for ST-S: [H_2S/600 °C], and 24.3 nm for ST-S: [SO_2/600 °C]. This result shows that a change in the sulfur-containing gas environment during exfoliation of the graphene oxide may affect the density of defects in the material and hence its resulting crystalline size. It was observed that undoped ST

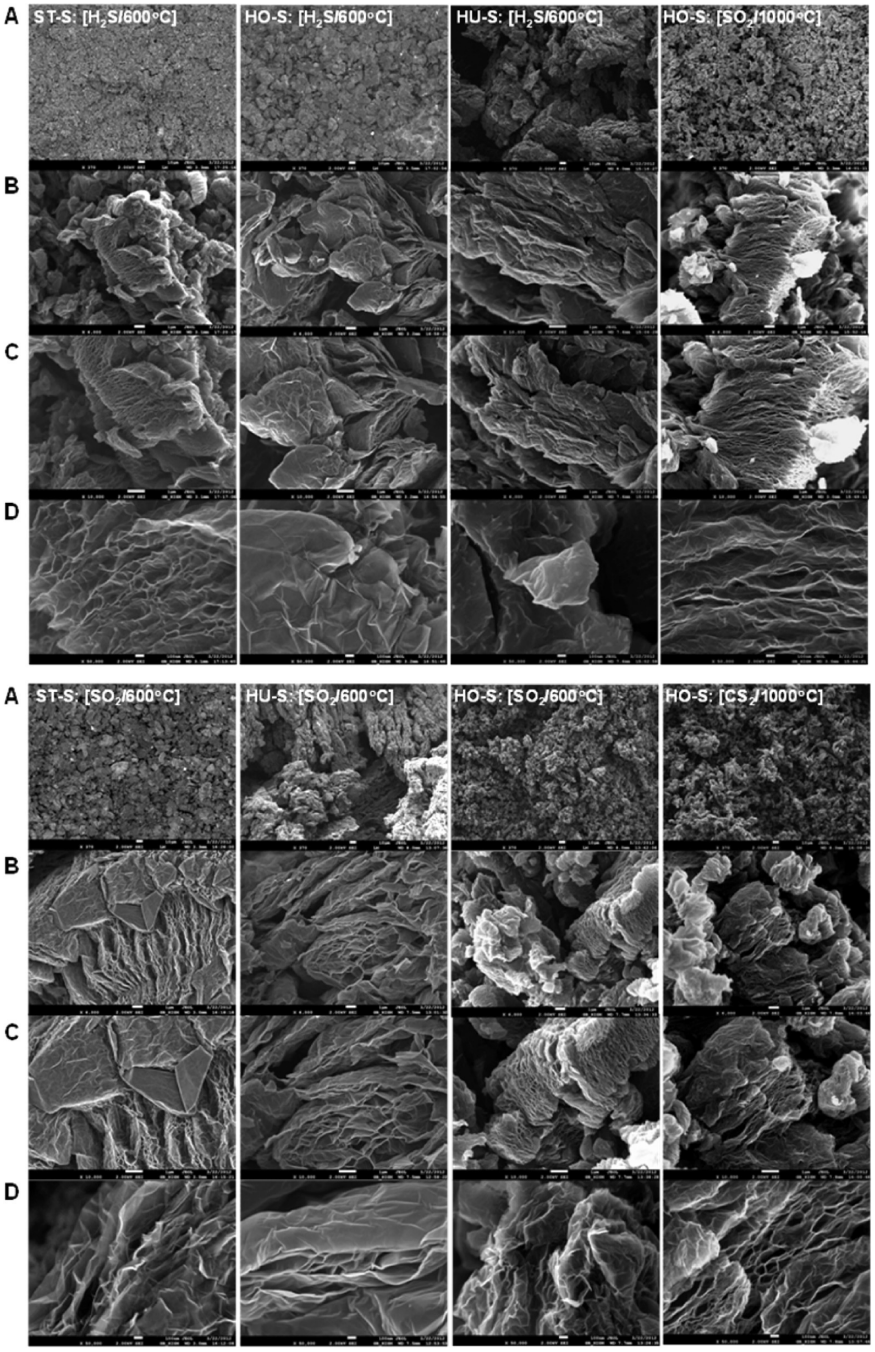

Figure 1. Scanning electron micrographs of sulfur-doped graphenes prepared from Hofmann, Hummers, and Staudenmaier graphite oxides by exfoliation in sulfur-containing gas at various temperatures. Magnification of (A) 370×, (B) 6000×, (C) 10 000×, and (D) 50 000×. Scale bars of 100 nm (A), 1 μm (B,C), and 10 μm (D).

possesses the highest D/G ratio as compared to the two other sulfur-doped graphene oxides.

Similarly, Raman spectroscopic measurements were also performed to obtain D/G band intensities for sulfur-doped graphene oxides using Hofmann synthesized graphite oxides as the starting material (as shown in Figure 2B,D). The measured D/G ratios are 1.09, 0.84, 0.85, 0.81, and 0.91 for HO, HO-S: [H_2S/600 °C], HO-S: [SO_2/1000 °C], HO-S: [SO_2/600 °C], and HO-S: [CS_2/1000 °C], respectively. Once again, the undoped thermally reduced graphene oxide (HO) displays a higher D/G ratio as compared to the S-doped HO materials where similar phenomenon was also observed in the case of ST materials. The use of H_2S and SO_2 sources as the dopant resulted in similar D/G ratios of approximately 0.83, except for CS_2, which gives an exceptionally high reading of 0.91 among the three different sulfur-doping sources. Average crystalline sizes of these materials were calculated to be 15.4, 20.0, 19.7, 20.8, and 18.5 nm for HO, HO-S: [H_2S/600 °C], HO-S: [SO_2/1000 °C], HO-S: [SO_2/600 °C], and HO-S: [CS_2/1000 °C], respectively. This result shows that

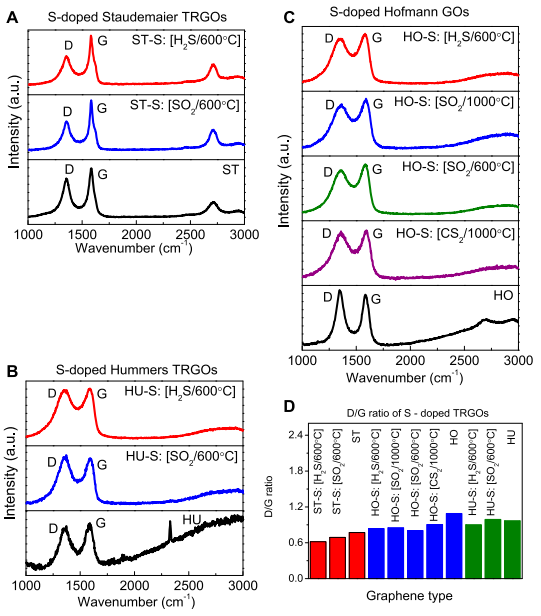

Figure 2. Raman spectra of sulfur-doped graphenes prepared from (A) Staudenmaier, (B) Hummers, and (C) Hofmann graphite oxides by exfoliation in sulfur-containing gas at various temperatures, as stated in the figure. Raman spectra of control materials exfoliated in inert gas are also shown. (D) D and G band intensity ratios.

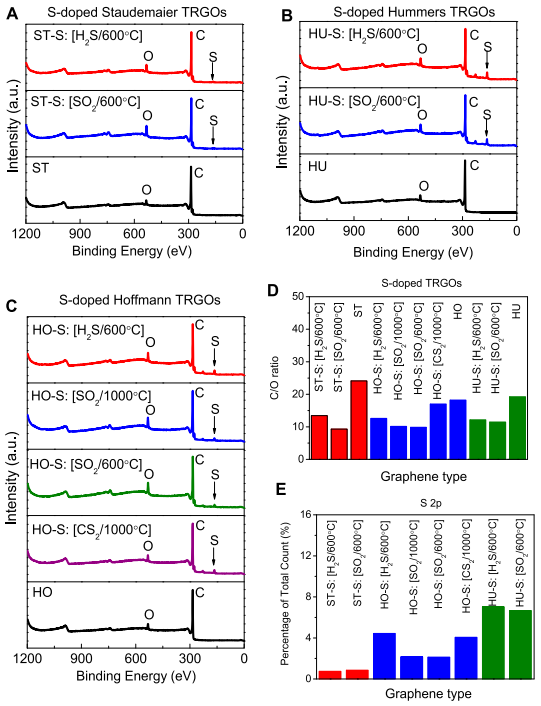

Figure 3. Wide-range XPS spectra of sulfur-doped graphenes prepared from (A) Staudenmaier, (B) Hummers, and (C) Hofmann graphite oxides by exfoliation in sulfur-containing gas at various temperatures, as stated in the figure. XPS spectra of control materials exfoliated in inert gas are also shown. (D) C 1s and O 1s (sensitivity factor corrected) ratios in particular graphenes. (E) Percentage of S 2p signal in total count of wide-angle XPS spectra.

sulfur-doped Hofmann graphene oxides have a larger crystalline structure as compared to non-sulfur-doped Hofmann graphene oxides. Sulfur-doping treatments were also performed on graphite oxides produced from Hummers method to give D/G ratios of 0.97 for HU, 0.90 for HU-S: [H_2S/600 °C], and 0.99 for HU-S: [SO_2/600 °C] (refer to Figure 2C,D). It can be observed from the results that sulfur-doped Hummers graphene oxides are found to consist of a higher amount of defects as compared to ST and HO sulfur-doped materials. D/G ratios were also used for the derivation of the average crystalline sizes, which are calculated to be 17.3 nm for HU, 16.9 nm for HU-S: [H_2S/600 °C], and 18.5 nm for HU-S: [SO_2/600 °C]. The Raman measurements obtained showed that the D/G ratio only displays a logical trend within each type of graphene oxide used for sulfur-doping treatments. However, a noncoherent trend exists between different types of graphene oxides that were doped under similar conditions. It could be clearly observed that all doped and undoped Hofmann graphene oxides possess the highest D/G ratios followed by HU graphene oxides (doped and undoped) and, finally, doped and undoped ST graphene oxides having the lowest D/G ratios of the three different types of materials. It should be noted that a small increase of background in Raman spectra is due to weak photoluminescence of the sample.[29]

Exfoliation of the three types of graphite oxides under different sulfur gaseous environments was performed in an attempt to successfully dope the materials' surfaces with sulfur. Therefore, it is crucial to study the surface composition of the materials to investigate the various functionalities present on the surface in order to determine the successful incorporation of sulfur into the materials. X-ray photoelectron spectroscopy utilizes a focused X-ray beam to irradiate the materials surface, obtaining the chemical composition information of the elements present *via* their respective electronic states. This measurement is presented as a form of a wide-range spectrum for the different materials, as shown in Figure 3, where the C 1s peak occurs at ~284.5 eV, O 1s at ~534 eV, and S 2p at ~167 eV. Figure 3A shows the XPS spectra of the ST and sulfur-doped ST materials where the presence of C and O could be clearly observed for all three materials. The existence of the S 2p peak at 167 eV for ST-S: [H_2S/600 °C] and ST-S: [SO_2/600 °C] coupled with the absence of the S 2p peak in the ST spectrum shows successful doping of the materials with sulfur. Further information on the degree of oxidation of the material can be obtained through the calculation of the C/O ratios with relative sensitivity factors taken into consideration. The intensities of the C 1s and O 1s peaks allow the derivation of a C/O ratio where a higher ratio indicates lesser oxygen functionalities on the surface and, hence, a more reduced material. Calculation of the C/O ratios shows that ST possesses a ratio of 24.09; ST-S: [H_2S/600 °C] has a value of 13.44, and ST-S: [SO_2/600 °C] has a value of 9.30. It was observed that

sulfur-exfoliated Staudenmaier graphene oxides have a lower C/O ratio as compared to undoped ST (refer to Figure 3D). This shows that the exfoliation of graphene oxides under a sulfur-containing gas environment results in the addition of oxygen functionalities on the materials' surfaces as compared to exfoliation under nitrogen gas environment. Further wide spectra XPS measurements were also carried out on HO graphite oxides exfoliated under a sulfur gaseous environment to investigate their respective C/O ratios.

As shown in Figure 3C, the spectra of sulfur-doped HO materials display the presence of a C 1s, O 1s, and S 2p peak at similar respective binding energies as the peaks shown earlier for sulfur-doped ST materials. The control material HO once again exhibits only a C 1s and an O 1s peak, and hence, the absence of the S 2p is a clear indication of the successful incorporation of sulfur into the exfoliated HO graphene oxides. The calculated C/O ratios for HO materials are 18.23 for HO, 12.61 for HO-S: [H_2S/600 °C], 10.17 for HO-S: [SO_2/1000 °C], 9.86 for HO-S: [SO_2/600 °C], and 17.02 for HO-S: [CS_2/1000 °C]. It can be observed from these values that all sulfur-doped HO graphene oxides have lower C/O ratios than the control material HO (refer to Figure 3D). This indicates that exfoliation under a sulfur gaseous environment results in the inclusion of more oxygen functionalities onto the graphene oxides surfaces as compared to a nitrogen gaseous environment. This phenomenon was also observed earlier for ST materials where the control material, ST, was found to have a much higher C/O ratio than its sulfur-doped counterparts. Among the four doped HO graphene oxides, doping of the graphene oxide using CS_2 as the sulfur source proved to have the highest C/O ratio. This indicates that exfoliation of HO graphite oxide in a CS_2 gaseous environment results in a larger extent of elimination of the oxygen moieties from graphene oxide's surface as compared to exfoliation in other sulfur sources. These results are in good agreement with the results obtained from ζ-potential measurement, which will be further elaborated in a later section. Wide-range XPS scans for doped and undoped HU graphene oxides were recorded, as shown in Figure 3B, where the C 1s, O 1s, and S 2p peaks are observed at binding energies of ∼285, ∼535, and ∼167 eV, respectively, similar to the values reported earlier for HO and ST materials. Presence of a S 2p peak in the spectra for sulfur-doped HU as compared to the absence of a S 2p peak in undoped HU graphene oxide is evidence of the successful incorporation of sulfur during exfoliation of the material. Calculation of the intensities of the C 1s and O 1s peaks gives the following C/O ratios (refer to Figure 3D) of 19.28 for HU, 12.19 for HU-S: [H_2S/600 °C], and 11.49 for HU-S: [SO_2/600 °C]. Similarly, undoped graphene oxides possessed higher C/O ratios than their sulfur-doped counterparts, where this same trend was observed for HO and ST materials.

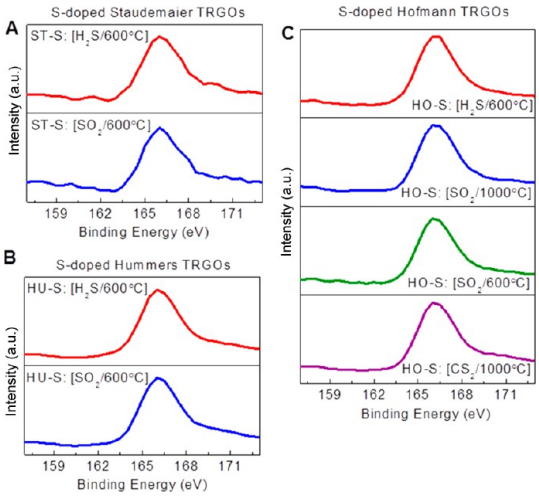

Figure 4. High-resolution XPS spectra of the S 2p signal of sulfur-doped graphenes prepared from (A) Staudenmaier, (B) Hummers, and (C) Hofmann graphite oxides by exfoliation in sulfur-containing gas at various temperatures. XPS spectra of control materials exfoliated in inert gas are also shown.

This shows that the phenomenon of an addition of oxygen functionalities in the materials during exfoliation occurred not only for HO and ST but also for HU materials. Similarly, no obvious trend could be observed in the comparison between different graphene oxides exfoliated under similar sulfur environment and conditions.

A more significant observation was realized in the comparison within each type of graphene oxides, such as Staudenmaier, Hummers, and Hofmann, as discussed in the earlier section. The intensities of the S 2p peaks are plotted in the form of a bar graph, as shown in Figure 3E, as a percentage of the total number of counts collected during the XPS measurement. The total amount of S is calculated as a percentage of the total elemental composition at the materials' surfaces. The percentages are reported to be 0.75 for ST-S: [H_2S/600 °C] and 0.87 for ST-S: [SO_2/600 °C] for ST materials. HO materials are observed to have percentages of 4.44 for HO-S: [H_2S/600 °C], 2.16 for HO-S: [SO_2/1000 °C], 2.13 for HO-S: [SO_2/600 °C], and 4.07 for HO-S: [CS_2/1000 °C]. HU materials were also recorded to have the following percentages of 7.03 for HU-S: [H_2S/600 °C] and 6.67 for HU-S: [SO_2/600 °C]. It could be observed that sulfur-doped Hummers materials possessed the highest sulfur content, followed by sulfur-doped Staudenmaier and last Hofmann materials. It is of interest to highlight that the extent of S doping in graphene is more dependent on the type of graphite oxide used than on the type of sulfur gas atmosphere utillized during synthesis. This is of great significance as ST, HO, and HU graphite/graphene oxides are frequently used interchangeably in several reports in the literature without any emphasis on the fact that they are actually very different materials.[30]

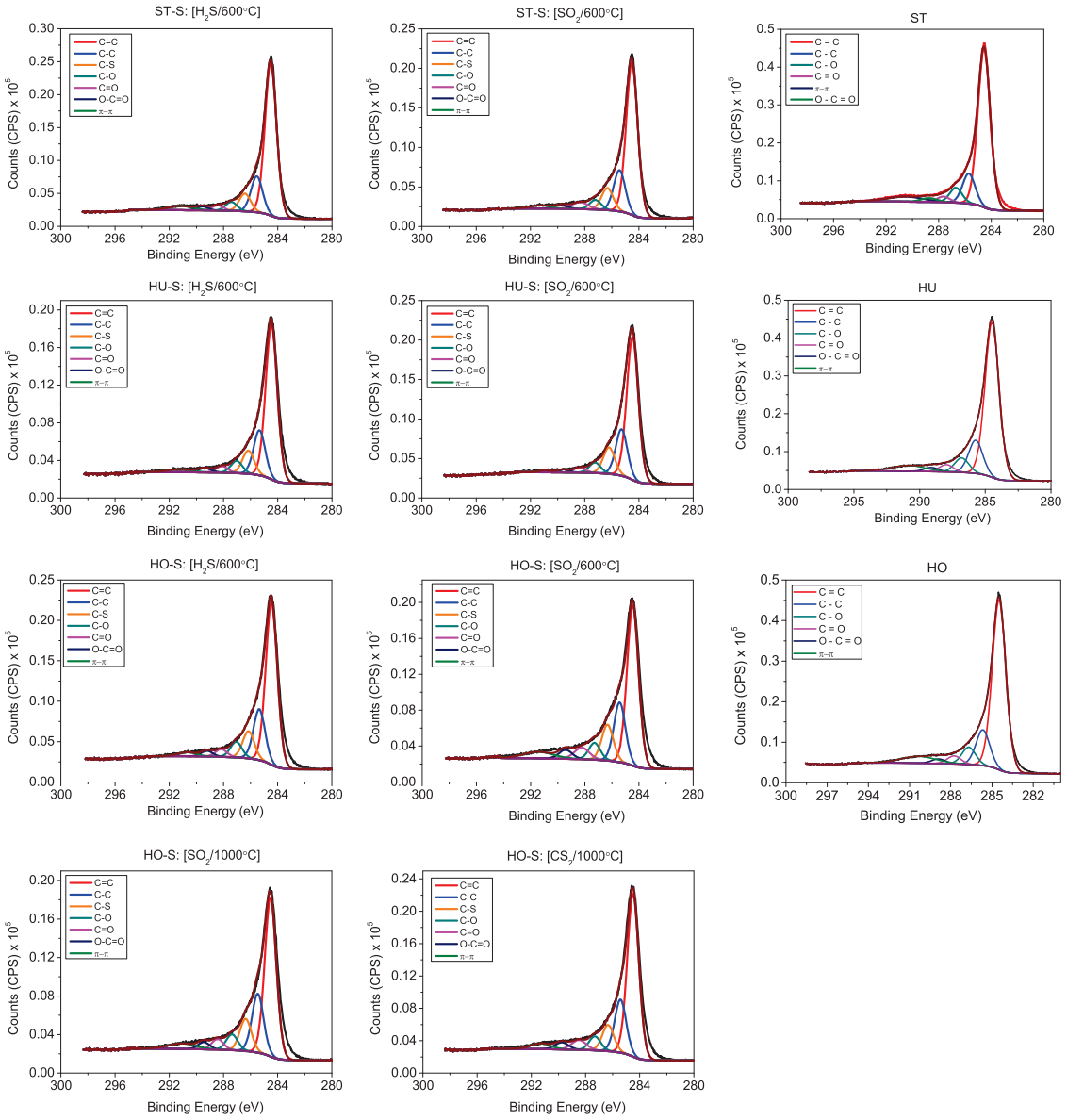

Figure 5. High-resolution XPS spectra of C 1s signal of sulfur-doped graphenes prepared from Staudenmaier (ST), Hummers (HU), and Hofmann (HO) graphite oxides by exfoliation in sulfur-containing gas at various temperatures. XPS spectra of control materials exfoliated in inert gas are also shown.

Crucial information on the types of oxygen and sulfur-containing groups present in each material is important in the characterization of the materials. It allows a complete understanding of the synthesis process and how each functional group is incorporated into the materials' surfaces during the synthesis step. The identification of these functionalities can be achieved through a high-resolution X-ray photoelectron spectroscopic measurement for a specific electronic state of the element of interest at their respective range of binding energies. HR-XPS scans were performed for S 2p and C 1s electronic states at approximately 167 and 284.5 eV, respectively, for all of the materials, as shown in Figure 4 (for sulfur-bonded species *via* S 2p signal) and Figure 5 (for carbon-bonded species *via* C 1s signal). High-resolution XPS scans were obtained for the sulfur-doped graphene oxides at the S 2p electronic state, as shown in Figure 4, at the binding energy of approximately 167 eV. HR-XPS measurements were carried out for sulfur-doped ST materials, sulfur-doped HU, and sulfur-doped HO, as shown in Figure 4A–C, respectively. All of the S 2p spectra show a single broad symmetrical peak at the position 167 eV, indicating the existence of a single type of S bonding interaction in the structure. With the S 2p peak's maximum intensity positioned at 167 eV, this peak can be concluded to be attributed to the presence of sulfur in the S^{6+} valence state, which indicates the presence of a SO_3H group.[31] These observations were also confirmed by the ζ-potential measured and the FT-IR spectra obtained for the materials (Figure 6 and Supporting Information Figure S1, respectively). Interestingly, the presence of SO_3H group was also observed

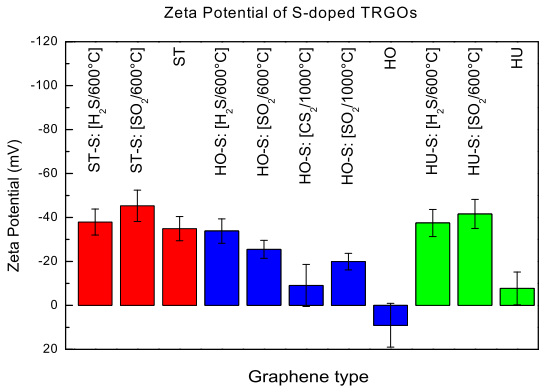

Figure 6. Zeta-potentials of sulfur-doped graphenes prepared from Staudenmaier (ST), Hummers (HU), and Hofmann (HO) graphite oxides by exfoliation in sulfur containing gas at various temperatures. Values of ζ-potential of control materials exfoliated in inert gas are also shown.

for samples exfoliated in H_2S and CS_2 atmosphere (see Figure S1, Supporting Information). In this case, the hydrogen sulfide acts as a reducing agent in the reaction with graphite oxide where sulfur is oxidized to higher valence state and is covalently bonded to the graphene. This observation is confirmed by the higher C/O ratio measured by XPS and combustion elemental analysis, which will be discussed later. On the other hand, the sulfur dioxide acts as an oxidizing agent as much lower C/O ratios are observed on samples exfoliated in SO_2 atmosphere. At high temperatures (1000 °C), the exfoliation in SO_2 atmosphere led to an oxidation of exfoliated graphene.

HR-XPS scans were also performed for the C 1s electronic state at approximately 284.5 eV to investigate the types of oxygen- and sulfur-containing groups present on the surface of these materials (Figure 5). Fitting of the C 1s spectrum was carefully performed to identify and quantify the various possible carbon interactions that may be present on the material's surface. It was observed that all undoped reduced graphene oxides (ST, HU, HO) display six carbon interactions at 284.5 eV for C═C, 285.7 eV for C−C, 286.8 eV for C−O, 288.0 eV for C═O, 289.2 eV for O−C═O, and 290.8 eV for $\pi-\pi$ interactions. The spectrum is often shown as a symmetrical peak at 284.5 eV, which corresponds to C═C interaction and a trailing tail shape at higher binding energy which depicts the $\pi-\pi$ interaction (refer to Figure 5). On the other hand, all sulfur-doped graphene oxides also exhibited all six carbon interactions that were previously observed for undoped graphene oxides at their respective binding energies that are similar to the values reported above. The appearance of a C−S peak was also detected at approximately 286.5 eV, which is of a lower energy than the C−O interaction due to oxygen being more electronegative which results in C−O displaying stronger charging behavior. The presence of the C−S peak indicates not only the successful inclusion of sulfur during exfoliation but also implications that the S exists inside the lattice structure of the graphene and is covalently bonded to the graphene.

Compared to high surface sensitivity of XPS, the combustible elemental analysis gives information about the "bulk" composition of material. The results obtained from elemental analysis measurements are in agreement with the data obtained from XPS. The highest concentration of sulfur content was found to be present in the samples prepared from graphite oxide prepared by the Hummers method (11.99 wt % S in HU-S: [H_2S/600 °C] and 10.42 wt % S in HU-S: [SO_2/600 °C]). The second highest concentration of sulfur was detected in the samples prepared from GO according to Hofmann method (4.12 wt % in HO-S: [SO_2/1000 °C] and 3.69 wt % HO-S: [SO_2/600 °C]). Higher incorporation of sulfur was observed for samples exfoliated in atmospheres with low valence sulfur compounds—hydrogen sulfide and carbon disulfide. The concentrations of S in HO-GO exfoliated with these sulfur precursors were 8.37 wt % for HO-S: [H_2S/600 °C] and 7.34 wt % for HO-S: [CS_2/1000 °C]. The concentration of sulfur in ST-GO exfoliated in H_2S and SO_2 atmosphere was below 0.1 wt %. This observation can be explained by the incomplete formation of sulfur dioxide during combustion analysis. Sulfur dioxide formed during the combustion process is used for measurement of sulfur concentration within the sample. On the basis of this observation, we can make some general conclusions that the incorporation of sulfur is dependent on the degree of GO oxidation and, hence, the method of preparation of the GO. Sulfur precursors used during exfoliation have also significantly influenced the resultant composition percentages of graphene. Reactions with hydrogen sulfide and carbon disulfide with sulfur in the oxidation state 2− results in the material having a higher C/O ratio and also a higher concentration of sulfur. A complete list of the results from elemental analysis can be obtained in Table S1 (Supporting Information). These results are consistent with the observations obtained from the ζ-potential measurements for the materials.

Dispersions of TRGOs in water were analyzed by measuring their ζ-potential (Figure 6). Sulfur-doped ST reduced by hydrogen sulfide and sulfur dioxide exhibited slightly higher (in absolute values) ζ-potential (−38 and −45 mV, respectively) compared to the TRGO in nitrogen (−35 mV). This could be due to the bonding of sulfonic acid group ($-SO_3H$) to the graphene framework. As the concentration of sulfur in the materials is low (refer to XPS and elemental analysis results), ζ-potential is most likely to be influenced by the oxygen functionalities found in the materials. In the comparison within sulfur-doped and undoped HO TRGOs, a different trend can be observed. Undoped TRGO that is exfoliated in an inert gas atmosphere exhibited a very distinct ζ-potential of +9 mV,

TABLE 1. Numerical Data of Conductivities of Sulfur-Doped Graphenes

Sample	Resistivity (Ω.cm)
ST-S: [H_2S/600°C]	5.5×10^{-5}
ST-S: [SO_2/600°C]	4.1×10^{-5}
ST: [N_2/1000°C]	5.1×10^{-5}
HO-S: [H_2S/600°C]	5.9×10^{-4}
HO-S: [SO_2/600°C]	5.2×10^{-4}
HO-S: [CS_2/1000°C]	3.4×10^{-4}
HO-S: [SO_2/1000°C]	5.9×10^{-4}
HO: [N_2/1000°C]	3.9×10^{-4}
HU-S: [H_2S/600°C]	1.0×10^{-3}
HU-S: [SO_2/600°C]	1.2×10^{-3}
HU: [N_2/1000°C]	8.0×10^{-4}

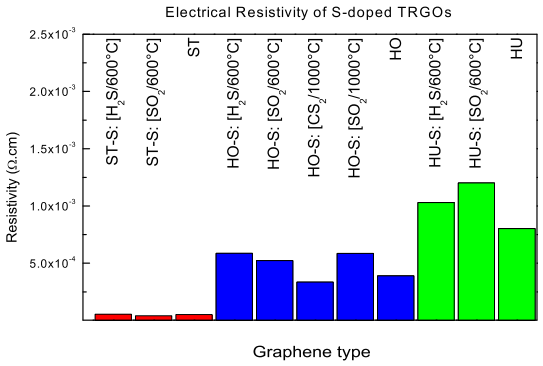

Figure 7. Electrical resistivity of sulfur-doped graphenes prepared from Staudenmaier (ST), Hummers (HU), and Hofmann (HO) graphite oxides by exfoliation in sulfur-containing gas at various temperatures. The values of resistivity of control materials exfoliated in inert gas are also shown.

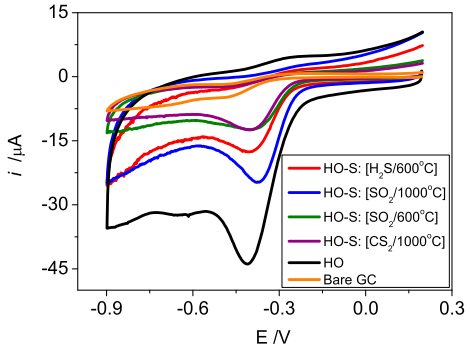

Figure 8. Cyclic voltammograms for undoped and sulfur-doped graphenes in O_2 saturated solution of 0.1 M KOH. Conditions: scan rate of 100 mV/s.

suggesting a very high degree of GO reduction in the material. The positive potential measured may be attributed to nitrogen contamination in the HO. TRGOs exfoliated in H_2S and SO_2 were observed to have more negative potentials of −34 mV for H_2S and −26 and −20 mV for SO_2 at 600 and 1000 °C, respectively. The highly negative potentials observed were likely to be attributed to $-SO_3H$ and oxygen groups present in the materials. Sulfur-doped HO in CS_2 exhibits lower ζ-potential of −9 mV even though it possessed similar elemental composition as HO doped by H_2S (according to XPS and elemental analysis results). Sulfur-doped HU was observed to have ζ-potentials (−38 mV for H_2S and −42 mV for SO_2) that were similar to those measured for sulfur-doped ST TRGOs. Undoped HU has a lower potential of −8 mV, similar to that of undoped HO. In conclusion, sulfur-doped TRGOs always exhibit higher values of ζ-potentials as compared to undoped TRGOs and, therefore, are more stable when dispersed in aqueous solutions. This behavior can be explained by the presence of two groups: acidic $-SO_3H$ group and unreduced oxygen groups. The presence of $-SO_3H$ group was expected for GO reduced in SO_2 but comes as a surprise in the case of H_2S. Earlier XPS results have shown the presence of $-SO_3H$ group (refer to XPS results Figure 4) where the position and fwhm of the S 2p peak were the same for all sulfur-doped samples. The peaks were centered at 166.3 eV, which suggests oxidized sulfur with a valence of 6+. It is interesting to note that no thiol group (−SH) was detected for GO reduced with hydrogen sulfide (~162 eV). Similarly, the preference to create sulfonic groups and not thiol groups was observed on carbon chain when doping with thiol precursor as shown in earlier studies.[31] Both XPS and elemental analysis results have confirmed that a higher concentration of oxygen was present in GO reduced by SO_2 than in GO reduced by H_2S. This observation was anticipated as the SO_2 groups contain oxygen atoms that contributed to the oxygen content while H_2S has to react with oxygen groups in GO in order to form $-SO_3H$.

Consequently, we have measured the resistivity of sulfur-doped graphene oxides as well as undoped graphene oxides exfoliated in inert gas atmosphere (refer to Table 1 and Figure 7). Majority of the sulfur-doped samples showed higher resistivity than their undoped counterparts that were reduced in nitrogen atmosphere. The increase in their resistivities can be attributed to the trapping of free carriers by the sulfur and oxygen functionalities. Such similar influence on the resistivity was also observed for the GO exfoliated in the presence of halogens.[13]

It has been previously reported that sulfur-doped graphenes can act as metal-free electrocatalysts for oxygen reduction.[21] In order to investigate electrocatalytic activity of sulfur-doped graphene toward oxygen reduction, we performed cyclic voltammetry of solution saturated with O_2 in 0.1 M KOH (Figure 8). We have found that O_2 reduction on a bare glassy carbon electrode requires large overpotentials (peak potential of −492 mV *vs* Ag/AgCl); undoped graphene (HO)

results in lower overpotentials required (peak potential of −411 mV *vs* Ag/AgCl). Sulfur-doped graphenes provided excellent electrocatalytic surfaces, being able to reduce oxygen at −405 mV for HO-S: [H_2S/600 °C], −397 mV for HO-S: [CS_2/1000 °C], −380 mV for HO-S: [SO_2/600 °C], and even only −370 mV for HO-S: [SO_2/1000 °C]. The shift of reduction potential by 40 mV from −411 to −370 mV from undoped graphene to S-doped graphene shows that sulfur-doped graphenes provide electrocatalytic surface of O_2 reduction reaction.

CONCLUSION

Doping of graphene with sulfur was made possible using various sulfur sources and reaction conditions to give final products with different amounts of sulfur content. This synthesis procedure was carried out with three main graphite oxide sources: Staudenmaier, Hummers, and Hofmann. We have investigated the physical and chemical properties of these materials in an attempt to understand how the variation in the reaction conditions has impacted the final outcome of these materials. Physical properties of these materials were studied using scanning electron microscopic technique where all of the sulfur-doped graphene oxides were found to be fully exfoliated, similar to the undoped graphene oxides. Raman spectroscopy results showed that all undoped graphene oxides possessed higher defect density than their sulfur-doped counterparts with the exception of HU. S-doped HO materials were also found to have the highest amount of defects followed by HU and eventually ST materials. XPS measurements and elemental combustible analysis have shown that HU has the highest sulfur content followed by HO and finally ST materials. The ζ-potential measurements showed that sulfur doping has a significant effect on the water dispersion stability of the sulfur-doped GO. All sulfur-doped materials exhibit higher (absolute value) ζ-potentials than their undoped counterparts. Especially, ST and HU S-doped GO treated with SO_2 have good dispersion stability (ζ-potential over −40 mV, generally considered limit for "good stability"). This is in accordance with the expectations that the sulfur is present as a $-SO_3H$ group. The ζ-potential is determined both by the type of graphite oxide starting material and by the exfoliation atmosphere. Especially S-doped HO and HU exhibited strong increase of their ζ-potentials as compared to undoped HO and HU. There is also a good correlation between the concentration of sulfur and the increase of ζ-potential. The concentration of sulfur in S-doped ST, as evaluated from the XPS, was lowest of the graphite oxides, and the corresponding shift of ζ-potential was least significant. The resistivity measurements confirmed the electron trapping ability of the sulfur dopant. Majority of the S-doped GO materials show higher resistivity than their undoped counterparts. However, the absolute values are still determined by the oxidation method rather than by the exfoliation atmosphere. The combustible elemental analysis is in good agreement with the XPS results. It confirmed that the highest concentration of sulfur was found for S-doped HU materials. The concentrations of sulfur also correspond with the ζ-potential results and the possibility of a sulfonic group present on the surface of the graphene oxides. The concentration of oxygen is also in accordance with the XPS results and suggests that graphite oxides treated with SO_2 have a higher degree of oxidation than those exfoliated in more reducing atmospheres (N_2, H_2S, CS_2). We have demonstrated that sulfur-doped graphenes exhibit electrocatalytic behavior for oxygen reduction reaction.

EXPERIMENTAL PROCEDURE

Materials. Sulfuric acid (98%), nitric acid (68%), nitric acid (fuming, 98%), potassium chlorate (98%), potassium permanganate (98%), hydrogen peroxide (30%), hydrochloric acid (37%), silver nitrate (99.5%), and barium nitrate (99.5%) were obtained from PENTA, Czech Republic. Carbon disulfide (99.9%) and *N*,*N*-dimethylformamide (DMF) were obtained from Aldrich. Graphite microparticles (<50 μm) were obtained from KOOH-I-NOOR Grafit, Czech Republic. The gases were obtained from SIAD (nitrogen 99.9999% and hydrogen sulfide 99.5%) and Linde (sulfur dioxide 99.98%).

Apparatus. Scanning electron microscopic (SEM) images were acquired using a JEOL 7600F field-emission scanning electron microscope (JEOL, Japan) at 5 kV accelerating voltage. Preparation of the samples was performed by attaching the materials onto a sticky conductive carbon tape which was then mounted onto an aluminum sample stub. X-ray photoelectron spectroscopy (XPS) measurement was executed with a Phoibos 100 spectrometer and a monochromatic Mg X-ray radiation source (SPECS, Germany) for the wide-range and high-resolution C 1s scans at 12.53 kV. The XPS samples were prepared by attaching a uniform layer of the materials onto a conductive carbon tape which was then affixed onto an aluminum XPS sample holder. The C/O ratios were achieved from the wide-scan XPS measurements with relative sensitivity factors taken into consideration during calculations. Raman spectroscopy was performed with a confocal micro-Raman LabRam HR instrument (Horiba Scientific) in backscattering geometry with a CCD detector. A 514.5 nm Ar laser and an Olympus optical microscope with a 100× objective lens were used in the focusing of the samples. Calibration of the machine was carried out at 0 and 520 cm^{-1} with a silicon wafer as reference to give a peak position resolution of less than 1 cm^{-1}. All samples were well-compressed and compacted before placing on top of a glass slip which was positioned on a piece of glass slide before any actual measurement was carried out. The elemental analysis (CHNS-O) was performed with Vario EL III (Elementar Analysensysteme GmbH, Germany). The calibration was performed with 5 mg of 4-aminobenzenesulfonic acid. The measurements of ζ-potential were performed on Malvern Zetasizer Nano ZS. Diluted samples of 1 mg of TRGO/25 mL of H_2O mass concentration were first ultrasonicated for 5 min and then measured in a folded capillary cell at pH 7. For electrical resistivity measurements of graphene materials, 40 mg of the powder material was first compressed into a capsule (1/4 in. diameter) under a pressure of 400 MPa for 30 s. The resistivity of

the resulting capsule was measured by a four-probe technique using the Van der Pauw method.[32] The resistivity measurements were then performed with Keithley 6220 current source and Agilent 34970A data acquisition/switch unit. The measuring current was set to 10 mA. The FT-IR measurement was performed on Bruker IFS 66v spectrometer equipped with IR microscope Hyperion. Germanium ATR crystal and liquid nitrogen cooled MCT detector were used for the measurements. Electrochemical measurements were carried out at Autolab 302 (EcoChemie), using a three-electrode setup. Glassy carbon working electrode (GC), platinum auxiliary electrode (Pt) with a diameter of 3 mm, and Ag/AgCl reference electrode were obtained from Autolab, The Netherlands.

Synthesis Procedure of Staudenmaier Graphite Oxide[25]. The synthesis of ST-GO was performed according to the procedure reported previously. First, 87.5 mL of sulfuric acid (98%) and 27 mL of nitric acid (98%) were first cooled to 0 °C before 5 g of graphite was added to the mixture. The reaction mixture was then intensively stirred while 55 g of potassium chlorate were added over a period of 30 min. The reaction flask was then loosely capped to allow the escape of chlorine dioxide gas. The mixture was continuously stirred for 96 h at room temperature and then poured into 3 L of deionized water. After decantation, the graphite oxide was redispersed in 5% hydrochloric acid. The graphite oxide was decanted from hydrochloric acid and repeatedly centrifuged and redispersed until a negative reaction for chloride and sulfate ions (with $Ba(NO_3)_2$ and $AgNO_3$) was observed. Graphite oxide slurry was finally dried in a vacuum oven at 60 °C for 48 h before further use.

Synthesis Procedure of Hofmann Graphite Oxide[26]. The synthesis of HO-GO was performed according to the standard method reported in literature. First, 87.5 mL of sulfuric acid (98%) and 27 mL of nitric acid (68%) were first cooled to 0 °C before 5 g of graphite was dispersed into the reaction mixture by vigorous stirring. Keeping the reaction mixture vigorously stirred at 0 °C, $KClO_3$ (55 g) was then added over a period of 30 min. The reaction mixture was loosely capped to allow the escape of gaseous reaction products (ClO_2) and stirred at room temperature for 96 h. Upon completion of reaction, the mixture was poured into 3 L of deionized water and decanted. The reaction product was then redispersed in 2 L of 5% HCl and decanted. Graphite oxide was then repeatedly centrifuged and redispersed in deionized water until a negative reaction on sulfate and chloride ions (with $Ba(NO_3)_2$ and $AgNO_3$, respectively) was achieved. Graphite oxide slurry was finally dried in a vacuum oven at 60 °C for 48 h before further use.

Synthesis Procedure of Hummers Graphite Oxide[27]. The synthesis of HU-GO was performed according to the method reported previously. First, 115 mL of sulfuric acid (98%) was cooled to 0 °C and then 5 g of graphite and 2.5 g of $NaNO_3$ were added to the mixture. While vigorously stirred, 15 g of $KMnO_4$ was added over a period of 2 h. The reaction mixture was then removed from the cooling bath and stirred at room temperature for 4 h. The reaction mixture was then heated to 35 °C for 30 min, poured into 250 mL of deionized water, and heated to 70 °C. After 15 min, the mixture was poured into 1 L of deionized water. Unreacted $KMnO_4$ was decomposed with 10% hydrogen peroxide. The reaction mixture was then decanted and repeatedly centrifuged and redispersed until a negative reaction for sulfate ions (with $Ba(NO_3)_2$) was achieved. Graphite oxide slurry was then dried in a vacuum oven at 60 °C for 48 h before further use.

Synthesis Procedure of Sulfur-Doped Staudenmaier, Hummers, and Hofmann Graphite Oxide. All of the sulfur-doped graphene oxides were exfoliated in the same reactor as the thermally reduced graphene oxides. For every reaction, 100 mg of the graphite oxide starting material was inserted into a quartz glass capsule covered by sintered quartz glass filter facing the direction of the gas flow. The capsule was then attached to a magnetic manipulator and placed into a quartz horizontal reactor in the furnace. Before the placement of the sample into the hot zone of the reactor, the whole system was repeatedly evacuated and filled up with nitrogen. A mixture of nitrogen and sulfur precursor was used for the sulfonation process. First, the nitrogen flow (1 L/min) and the sulfur precursor (*i.e.*, SO_2 and H_2S) flow (1 L/min) were stabilized for 5 min. Then the capsule with the sample was inserted into the furnace for 12 min and pulled out again at the end of the reaction. In the case of samples treated in SO_2 at 1000 °C, the exposition time was reduced to 2 min in order to avoid oxidation and decomposition of graphene. The 12 min exposure of graphene at these conditions led to a complete oxidation. The reaction with CS_2 was carried out using a bubbler filled with liquid CS_2 at a temperature of 17 °C and pressure of 1000 mbar. Nitrogen (100 mL/min) was used as a carrier gas and was diluted with 1 L/min of nitrogen before entering into the reactor. All exfoliation steps were performed under atmospheric pressure.

Conflict of Interest: The authors declare no competing financial interest.

Acknowledgment. M.P. thanks MINDEF/NTU fund JPP 11/02/06 and JSPS-NTU fund. Z.S. and P.Š. thank the Ministry of Education of the Czech Republic (Project No. MSM6046137302) and the Specific University Research grant (MSMT No. 20/2013).

Supporting Information Available: Additional figures and table as described in the text. This material is available free of charge *via* the Internet at http://pubs.acs.org.

REFERENCES AND NOTES

1. Novoselov, K. S.; Geim, A. K.; Morozov, S. V.; Jiang, D.; Zhang, Y.; Dubonos, S. V.; Grigorieva, I. V.; Firsov, A. A. Electric Field Effect in Atomically Thin Carbon Films. *Science* **2004**, *306*, 666–669.
2. Geim, A. K.; Novoselov, K. S. The Rise of Graphene. *Nat. Mater.* **2007**, *6*, 183–191.
3. Rogers, J. A. Electronic Materials: Making Graphene for Macroelectronics. *Nat. Nanotechnol.* **2008**, *3*, 254–255.
4. Stankovich, S.; Dikin, D. A.; Dommett, D. H. B.; Kohlhaas, K. M.; Zimney, E. J.; Stach, E. A.; Piner, R. D.; Nguyen, S. T.; Ruoff, R. S. Graphene-Based Composite Materials. *Nature* **2006**, *442*, 282–286.
5. Ramanathan, T.; Abdala, A. A.; Stankovich, S.; Dikin, D. A.; Herrera-Alonso, M.; Piner, R. D.; Adamson, D. H.; Schniepp, H. C.; Chen, X.; Ruoff, R. S. Functionalized Graphene Sheets for Polymer Nanocomposites. *Nat. Nanotechnol.* **2008**, *3*, 327–331.
6. Stoller, M. D.; Park, S.; Zhu, Y.; An, J.; Ruoff, R. S. Graphene-Based Ultracapacitors. *Nano Lett.* **2008**, *8*, 3498–3502.
7. Liu, Z.; Robinson, J. T.; Sun, X.; Dai, H. PEGylated Nano-Graphene Oxide for Delivery of Water Insoluble Cancer Drugs. *J. Am. Chem. Soc.* **2008**, *130*, 10876–10877.
8. Rao, C. N. R.; Sood, A. K.; Subrahmanyam, K. S.; Govindaraj, A. Graphene: The New Two-Dimensional Nanomaterial. *Angew. Chem., Int. Ed.* **2009**, *48*, 7752–7777.
9. Pumera, M. Graphene-Based Nanomaterials and Their Electrochemistry. *Chem. Soc. Rev.* **2010**, *39*, 4146–4157.
10. Gutes, A.; Hsia, B.; Sussman, A.; Mickelson, W.; Zettl, A.; Carraro, C.; Maboudian, R. Graphene Decoration with Metal Nanoparticles: Towards Easy Integration for Sensing Applications. *Nanoscale* **2012**, *4*, 438–440.
11. Giovanni, M.; Poh, H. L.; Ambrosi, A.; Zhao, G.; Sofer, Z.; Sanek, F.; Khezri, B.; Webster, R. D.; Pumera, M. Noble Metal (Pd, Ru, Rh, Pt, Au, Ag) Doped Graphene Hybrids for Electrocatalysis. *Nanoscale* **2012**, *4*, 5002–5008.
12. Gopalakrishnan, K.; Subrahmanyam, K. S.; Kumar, P.; Govindaraj, A.; Rao, C. N. R. Reversible Chemical Storage of Halogens in Few-Layer Graphene. *RSC Adv.* **2012**, *2*, 1605–1608.
13. Poh, H. L.; Šimek, P.; Sofer, Z.; Pumera, M. Halogenation of Graphene with Chlorine, Bromine, or Iodine by Exfoliation in a Halogen Atmosphere. *Chem.—Eur. J.* **2013**, *19*, 2655–2662.
14. Zbořil, R.; Karlický, F.; Bourlinos, A. B.; Steriotis, T. A.; Stubos, A. K.; Georgakilas, V.; Šafářová, V.; Jančík, D.; Trapalis, C.; Otyepka, M. Graphene Fluoride: A Stable Stoichiometric Graphene Derivative and Its Chemical Conversion to Graphene. *Small* **2010**, *6*, 2885–2891.

15. Samarakoon, D. K.; Wang, X.-Q. Chair and Twist-Boat Membranes in Hydrogenated Graphene. *ACS Nano* **2009**, *3*, 4017–4022.
16. Wu, Z.-S.; Ren, W.; Xu, L.; Li, F.; Cheng, H.-M. Doped Graphene Sheets as Anode Materials with Superhigh Rate and Large Capacity for Lithium Ion Batteries. *ACS Nano* **2011**, *5*, 5463–5471.
17. Jin, Z.; Yao, J.; Kittrell, C.; Tour, J. M. Large-Scale Growth and Characterizations of Nitrogen-Doped Monolayer Graphene Sheets. *ACS Nano* **2011**, *5*, 4112–4117.
18. Reddy, A. L. M.; Srivastava, A.; Gowda, S. R.; Gullapalli, H.; Dubey, M.; Ajayan, P. M. Synthesis of Nitrogen-Doped Graphene Films for Lithium Battery Application. *ACS Nano* **2010**, *4*, 6337–6342.
19. Velez-Fort, E.; Mathieu, C.; Pallecchi, E.; Pigneur, M.; Silly, M. G.; Belkhou, R.; Marangolo, M.; Shukla, A.; Sirotti, F.; Ouerghi, A. Epitaxial Graphene on 4H-SiC(0001) Grown under Nitrogen Flux: Evidence of Low Nitrogen Doping and High Charge Transfer. *ACS Nano* **2012**, *6*, 10893–10900.
20. Qu, L.; Liu, Y.; Baek, J.-B.; Dai, L. Nitrogen-Doped Graphene as Efficient Metal-Free Electrocatalyst for Oxygen Reduction in Fuel Cells. *ACS Nano* **2010**, *4*, 1321–1326.
21. Yang, Z.; Yao, Z.; Li, G.; Fang, G.; Nie, H.; Liu, Z.; Zhou, X.; Chen, X.; Huang, S. Sulfur-Doped Graphene as an Efficient Metal-Free Cathode Catalyst for Oxygen Reduction. *ACS Nano* **2012**, *6*, 205–211.
22. Denis, P. A. Concentration Dependence of the Band Gaps of Phosphorus and Sulfur Doped Graphene. *Comput. Mater. Sci.* **2013**, *67*, 203–206.
23. Yan, Y.; Yin, Y.-X.; Xin, S.; Guo, Y.-G.; Wan, L.-J. Ionothermal Synthesis of Sulfur-Doped Porous Carbons Hybridized with Graphene as Superior Anode Materials for Lithium-Ion Batteries. *Chem. Commun.* **2012**, *48*, 10663–10665.
24. Wang, J.-Z.; Lu, L.; Choucairc, M.; Stridec, J. A.; Xua, X.; Liu, H.-K. Sulfur-Graphene Composite for Rechargeable Lithium Batteries. *J. Power Sources* **2011**, *16*, 7030–7034.
25. Staudenmaier, L. Verfahren zur Darstellung der Graphitsäure. *Ber. Dtsch. Chem. Ges.* **1898**, *31*, 1481–1487.
26. Hofmann, U.; Konig, E. Untersuchungen über Graphitoxyd. *Z. Anorg. Allg. Chem.* **1937**, *234*, 311–336.
27. Hummers, W. S.; Offeman, R. E. Preparation of Graphitic Oxide. *J. Am. Chem. Soc.* **1958**, *80*, 1339.
28. Canado, L. G.; Takai, K.; Enoki, T.; Endo, M.; Kim, Y. A.; Mizusaki, H.; Jorio, A.; Coelho, L. N.; Magalhaes-Paniago, R.; Pimenta, M. A. General Equation for the Determination of the Crystallite Size La of Nanographite by Raman Spectroscopy. *Appl. Phys. Lett.* **2006**, *88*, 163106.
29. Cuong, T. V.; Pham, V. H.; Shin, E. W.; Chung, J. S.; Hur, S. H.; Kim, E. J.; Tran, Q. T.; Nguyen, H. H.; Kohl, P. A. Temperature-Dependent Photoluminescence from Chemically and Thermally Reduced Graphene Oxide. *Appl. Phys. Lett.* **2011**, *99*, 041905.
30. Chua, C. K.; Sofer, Z.; Pumera, M. Graphite Oxides: Effects of Permanganate and Chlorate Oxidants on the Oxygen Composition. *Chem.—Eur. J.* **2012**, *18*, 13453–13459.
31. Adam, L.; Oki, A.; Grady, T.; McWhinney, H.; Luo, Z. Preparation and Characterization of Sulfonic Acid-Functionalized Single-Walled Carbon Nanotubes. *Physica E* **2009**, *41*, 723–728.
32. Van der Pauw, L. J. A Method of Measuring Specific Resistivity and Hall Effect of Discs of Arbitrary Shape. *Philips Res. Rep.* **1958**, *13*, 1–9.